THE REMARKABLE ABILITY OF TURBULENCE MODEL EQUATIONS TO DESCRIBE TRANSITION

13-15 JANUARY 1992

by

David C. Wilcox
DCW Industries, Inc.
La Cañada, California

Abstract

This paper demonstrates how well the k-ω turbulence model describes the nonlinear growth of flow instabilities from laminar flow into the turbulent flow regime. Viscous modifications are proposed for the k-ω model that yield close agreement with measurements and with Direct Numerical Simulation results for channel and pipe flow. These modifications permit prediction of subtle sublayer details such as maximum dissipation at the surface, $k \sim y^2$ as $y \to 0$, and the sharp peak value of k near the surface. With two transition specific closure coefficients, the model equations accurately predict transition for an incompressible flat-plate boundary layer. The analysis also shows why the k-ε model is so difficult to use for predicting transition.

I. Introduction

There has been renewed interest in development of methods for predicting boundary-layer transition. Current interest in vehicles such as the National Aerospace Plane (NASP), for example, provides the impetus for developing accurate transition prediction tools. Furthermore, because hypersonic boundary layers rarely achieve momentum-thickness Reynolds numbers large enough to sustain fully-developed turbulence, even the post-transition region generally exhibits nontrivial viscous effects. Consequently, accurate low-Reynolds-number turbulence models are also needed.

The standard approach is to view development of a transition model and a low-Reynolds-number turbulence model as two separate issues. The strongest argument in favor of this approach is simply that all spectral effects are lost in the time-averaging process used by turbulence models. Tollmien-Schlichting waves, for example, cannot be distinguished by a turbulence-model. Since a given boundary layer is unstable to perturbations that fall in a specific range of frequencies, conventional turbulence models, which distinguish only magnitude and an average frequency, can never be certain if a given perturbation will actually cause transition. However, if we implement two separate models, one for the transition region and another for the developing turbulent region, achieving a smooth joining of the two models' predictions presents an additional complication.

This complication can be avoided if we view both issues as low-Reynolds-number phenomena that can be addressed in the context of a single model. The strongest argument for this approach is that we can use the same model to describe a smooth transition from laminar to fully turbulent flow, including the transitional region. This approach is plausible provided we restrict our applications to broad-band transition-triggering disturbances.

The research of Wilcox, et al[1-6] provides a great deal of support for the latter approach. Using a k-ω² turbulence model and transition-specific, low-Reynolds-number modifications, Wilcox simulated boundary-layer transition for a wide range of Mach numbers including pressure gradient, surface roughness, surface heating and cooling, and surface

mass transfer. The purpose of this paper is to build upon the work of Wilcox, et al, taking advantage of recent Direct Numerical Simulation (DNS) results in developing appropriate viscous modifications for the Wilcox[7] k-ω model. The scope of this paper is confined to incompressible flows.

For incompressible turbulent fluid flow, the complete set of equations that constitute the Wilcox k-ω two-equation model are as follows.

$$\frac{\partial u_j}{\partial x_j} = 0 \tag{1}$$

$$\frac{\partial}{\partial t}(\rho u_i) + \frac{\partial}{\partial x_j}(\rho u_j u_i) = \frac{\partial}{\partial x_j}[-p\delta_{ji} + \hat{\tau}_{ji}] \tag{2}$$

$$\frac{\partial}{\partial t}(\rho k) + \frac{\partial}{\partial x_j}(\rho u_j k) = \tau_{ij}\frac{\partial u_i}{\partial x_j} - \beta^*\rho\omega k$$
$$+ \frac{\partial}{\partial x_j}[(\mu + \sigma^*\mu_T)\frac{\partial k}{\partial x_j}] \tag{3}$$

$$\frac{\partial}{\partial t}(\rho\omega) + \frac{\partial}{\partial x_j}(\rho u_j\omega) = \alpha\frac{\omega}{k}\tau_{ij}\frac{\partial u_i}{\partial x_j} - \beta\rho\omega^2$$
$$+ \frac{\partial}{\partial x_j}[(\mu + \sigma\mu_T)\frac{\partial\omega}{\partial x_j}] \tag{4}$$

$$\hat{\tau}_{ij} = 2\mu S_{ij} + \tau_{ij} \tag{5}$$

$$\tau_{ij} = 2\mu_T S_{ij} - \frac{2}{3}\rho k\delta_{ij} \tag{6}$$

$$\mu_T = \alpha^*\rho k/\omega \tag{7}$$

$$S_{ij} = \frac{1}{2}[\frac{\partial u_i}{\partial x_j} + \frac{\partial u_j}{\partial x_i}] \tag{8}$$

In Equations (1-8), t is time, x_i is position vector, u_i is velocity, ρ is density, p is pressure, μ is molecular viscosity, and $\hat{\tau}_{ij}$ is the sum of molecular and Reynolds stress tensors. Also, δ_{ij} is the Kronecker delta, k is the turbulence kinetic energy, ω is specific dissipation rate, τ_{ij} is Reynolds stress tensor, and μ_T is eddy viscosity. The six parameters α, α*, ß, ß*, σ and σ* are closure coefficients whose values are given below.

$$\alpha^* = \frac{\alpha_o^* + Re_T/R_k}{1 + Re_T/R_k} \tag{9}$$

$$\alpha = \frac{5}{9} \cdot \frac{\alpha_o + Re_T/R_w}{1 + Re_T/R_w} \cdot (\alpha^*)^{-1} \tag{10}$$

$$\beta^* = \frac{9}{100} \cdot \frac{5/18 + (Re_T/R_\beta)^4}{1 + (Re_T/R_\beta)^4} \qquad (11)$$

$$\beta = 3/40 , \quad \sigma^* = \sigma = 1/2 \qquad (12)$$

$$\alpha_o^* = \beta/3 , \quad \alpha_o = 1/10 \qquad (13)$$

$$R_\beta = 8 , \quad R_k = 6 , \quad R_w = 2.7 \qquad (14)$$

where Re_T is turbulence Reynolds number defined by

$$Re_T = \rho k / (\omega \mu) \qquad (15)$$

Section II explains in detail how the turbulence model simulates transition, and justifies the form of the viscous modifications. Section III explains why the most popular low-Reynolds-number k-ϵ models are unsuitable for predicting transition. Section IV demonstrates how well the model performs for low-Reynolds-number channel flow and for pipe flow. Section V includes transition predictions for an incompressible flat-plate boundary layer. Section VI presents a summary of and conclusions drawn from the study.

II. Simulating Transition with Turbulence Model Equations

Turbulence model equations can be used to predict transition from laminar to turbulent flow, although most models predict transition to turbulence at Reynolds numbers that are at least an order of magnitude too low. To understand why and how the k-ω model predicts transition, consider the flat-plate boundary layer. For the k-ω model, the incompressible, two-dimensional boundary-layer form of the equations for k and ω is as follows.

$$u \frac{\partial u}{\partial x} + v \frac{\partial u}{\partial y} = \frac{\partial}{\partial y} [(\nu + \nu_T) \frac{\partial u}{\partial y}] \qquad (16)$$

$$u \frac{\partial k}{\partial x} + v \frac{\partial k}{\partial y} = \nu_T (\frac{\partial u}{\partial y})^2 - \beta^* \omega k + \frac{\partial}{\partial y} [(\nu + \sigma^* \nu_T) \frac{\partial k}{\partial y}] \qquad (17)$$

$$u \frac{\partial \omega}{\partial x} + v \frac{\partial \omega}{\partial y} = \alpha \frac{\omega}{k} \nu_T (\frac{\partial u}{\partial y})^2 - \beta \omega^2 + \frac{\partial}{\partial y} [(\nu + \sigma \nu_T) \frac{\partial \omega}{\partial y}] \qquad (18)$$

$$\nu_T = \alpha^* k / \omega \qquad (19)$$

where u and v are velocity components in the streamwise (x) and normal (y) directions, respectively, ν is kinematic molecular viscosity, and ν_T is kinematic eddy viscosity. We can most clearly illustrate how the model equations predict transition by rearranging terms in Equations (17) and (18) as follows.

$$u \frac{\partial k}{\partial x} + v \frac{\partial k}{\partial y} = P_k \beta^* \omega k + \frac{\partial}{\partial y} [(\nu + \sigma^* \nu_T) \frac{\partial k}{\partial y}] \qquad (20)$$

$$u \frac{\partial \omega}{\partial x} + v \frac{\partial \omega}{\partial y} = P_\omega \beta \omega^2 + \frac{\partial}{\partial y} [(\nu + \nu_T) \frac{\partial \omega}{\partial y}] \qquad (21)$$

The *net production per unit dissipation* for the two equations, P_k and P_ω, are defined by:

$$P_k = \frac{\alpha^*}{\beta^*} (\frac{\partial u/ \partial y}{\omega})^2 - 1 \qquad (22)$$

$$P_\omega = \frac{\alpha \alpha^*}{\beta} (\frac{\partial u/ \partial y}{\omega})^2 - 1 \qquad (23)$$

There are two important observations worthy of mention at this point. *First*, if the turbulence energy is zero, Equation (21) has a well-behaved solution. That is, when k = 0, the eddy viscosity vanishes and the ω equation uncouples from the k equation. Consequently, the k-ω model has a nontrivial laminar-flow solution for ω. *Second*, the signs of P_k and P_ω determine whether k and ω are amplified or reduced in magnitude. However, it is not obvious by inspection of Equations (22) and (23) how the signs of these terms vary with Reynolds number as we move from the plate leading edge to points downstream. We can make the variation obvious by rewriting Equations (22) and (23) in terms of the Blasius transformation.

Before we introduce the Blasius transformation, we must determine the appropriate scaling for ω. To do this, we note that close to the surface of a flat plate boundary layer, the specific dissipation rate behaves according to[7]

$$\omega \rightarrow \frac{6 \nu}{\beta y^2} \quad as \quad y \rightarrow 0 \qquad (24)$$

In terms of the Blasius similarity variable, η, defined by

$$\eta = y / (\nu x/U_\infty)^{1/2} \qquad (25)$$

where U_∞ is freestream velocity, the asymptotic behavior of ω approaching the surface is

$$\omega \rightarrow \frac{6 U_\infty}{\beta} \frac{1}{x} \frac{1}{\eta^2} \quad as \quad \eta \rightarrow 0 \qquad (26)$$

Consequently, we conclude that the appropriate scaling for ω in the Blasius boundary layer is given by

$$\omega = \frac{U_\infty}{x} W(x,\eta) \qquad (27)$$

where $W(x,\eta)$ is a dimensionless function to be determined as part of the solution. Hence, if we write the velocity in terms of dimensionless velocity, $F(x,\eta)$, i.e.,

$$u = U_\infty F(x,\eta) \qquad (28)$$

the *net production per unit dissipation* terms become

$$P_k = \frac{\alpha^*}{\beta^*} Re_x (\frac{\partial F/ \partial \eta}{W})^2 - 1 \qquad (29)$$

$$P_\omega = \frac{\alpha \alpha^*}{\beta} Re_x (\frac{\partial F/ \partial \eta}{W})^2 - 1 \qquad (30)$$

Thus, both P_k and P_ω increase linearly with Reynolds number, Re_x. From the exact laminar solution for $F(\eta)$ and $W(\eta)$ [the x dependence vanishes for the Blasius boundary layer], the maximum value of the ratio of $\partial F/ \partial \eta$ to W is given by

$$(\frac{\partial F/ \partial \eta}{W})_{max} \approx \frac{1}{300} \qquad (31)$$

Hence, as long as the eddy viscosity remains small compared to the molecular viscosity, we can specify the precise points where P_k and P_ω change sign. In general, using Equation (31), we conclude that the sign changes occur at the following Reynolds numbers.

$$(Re_x)_k = 9 \cdot 10^4 \frac{\beta^*}{\alpha^*} \tag{32}$$

$$(Re_x)_\omega = 9 \cdot 10^4 \frac{\beta}{\alpha\alpha^*} \tag{33}$$

With no viscous modifications, the closure coefficients α, α^*, β and β^* are 5/9, 1, 3/40 and 9/100, respectively. These values correspond to the limiting form of Equations (9-14) as $Re_T \to \infty$. Using these *fully turbulent* values, we find $(Re_x)_k = 8,100$ and $(Re_x)_\omega = 12,150$. Thus, starting from laminar flow at the leading edge of a flat plate, the following sequence of events occurs.

---

(1)   The computation starts in a laminar region with $k = 0$ in the boundary layer and a small freestream value of k.

(2)   Initially, because $P_k < 0$ and $P_\omega < 0$, dissipation of both k and ω exceeds production. Turbulence energy is entrained from the freestream and spreads through the boundary layer by molecular diffusion. Neither k nor ω is amplified and the boundary layer remains laminar.

(3)   At the *critical Reynolds number*, $Re_{x_c} = 8,100$, production catches dissipation in the k equation. Downstream of x_c, k production exceeds k dissipation and turbulence energy is amplified. At some point in this process, the eddy viscosity grows rapidly and this corresponds to the transition point.

(4)   k continues to be amplified and, beyond $Re_x = 12,150$ production catches dissipation in the ω equation. ω is now amplified and continues growing until a balance between production and dissipation is achieved in the k equation. When this balance is achieved, transition from laminar to turbulent flow is complete.

Consistent with experimental measurements, the entire process is very sensitive to the freestream value of k. There is also a sensitivity to the freestream value of ω, although the sensitivity is more difficult to quantify.

Three key points are immediately obvious. *First*, k begins growing at a Reynolds number of 8,100. By contrast, linear-stability theory tells us that Tollmien-Schlichting waves begin forming in the Blasius boundary layer at a Reynolds number of 90,000. This is known as the *minimum critical Reynolds number*. Correspondingly, we find that the model predicts transition at much too low a Reynolds number. *Second*, inspection of Equations (32) and (33) shows that the width of the transition region is controlled by the ratio of β to $\alpha\alpha^*$. *Third*, transition will never occur if P_ω reaches zero earlier than P_k. Thus, occurrence of transition requires

$$\alpha\alpha^* < \alpha^*\beta/\beta^* \quad \text{as} \quad Re_T \to 0 \tag{34}$$

This fact must be preserved in any viscous modification to the model. The viscous modifications in Equations (9-14), i.e., the dependence of α, α^* and β^* upon Re_T, are designed to accomplish two objectives. The most important

objective is to match the *minimum critical Reynolds number*. Reference to Equation (32) shows that we must require

$$\beta^*/\alpha^* \to 1 \quad \text{as} \quad Re_T \to 0 \tag{35}$$

A secondary objective is to achieve *asymptotic consistency* with the exact behavior of k and dissipation, $\epsilon = \beta^*k\omega$, approaching a solid boundary. That is, we would like to have

$$k/y^2 \to \text{constant}, \quad \epsilon/k \to 2\nu/y^2 \quad \text{as} \quad y \to 0 \tag{36}$$

Close to a solid boundary, Wilcox[7] shows that the dissipation and molecular diffusion terms balance in both the k and ω equations. The very-near-wall solution for ω is given by Equation (24). The solution for k is of the form

$$k/y^n \to \text{constant} \quad \text{as} \quad y \to 0 \tag{37}$$

where n is given by

$$n = \tfrac{1}{2}[1 + (1 + 24\beta^*/\beta)^{1/2}] \tag{38}$$

Noting that dissipation is related to k and ω by

$$\epsilon = \beta^*k\omega \tag{39}$$

we can achieve the desired asymptotic behavior of Equation (36) by requiring

$$\beta^*/\beta \to 1/3 \quad \text{as} \quad Re_T \to 0 \tag{40}$$

Requiring this limiting behavior as $Re_T \to 0$ is sufficient to achieve the desired asymptotic behavior as $y \to 0$ since the eddy viscosity, and hence, Re_T vanish at a solid boundary.

If we choose to have β constant for all values of Re_T, Equations (34), (35) and (40) are sufficient to determine the limiting values of α^* and β^* and an upper bound for $\alpha\alpha^*$ as turbulence Reynolds number becomes vanishingly small. Specifically, we find

$$\left.\begin{array}{rcl} \alpha\alpha^* & < & \beta \\[4pt] \alpha^* & \to & \beta/3 \\[4pt] \beta^* & \to & \beta/3 \end{array}\right\} \quad \text{as} \quad Re_T \to 0 \tag{41}$$

Wilcox, et al,[1-4] make the equivalent of $\alpha\alpha^*$ and α^* in their k-ω^2 models approach the same limiting value and obtain excellent agreement with measured transition width for incompressible boundary layers. Numerical experimentation with the k-ω model indicates the optimum choice for incompressible boundary layers is $\alpha\alpha^* \to 0.74\beta$, or

$$\alpha\alpha^* \to 1/18 \quad \text{as} \quad Re_T \to 0 \tag{42}$$

Equations (9-14) postulate functional dependencies upon Re_T that guarantee the limiting values in Equations (41) and (42), as well as the original *fully turbulent* values for $Re_T \to \infty$.

The three coefficients R_β, R_k and R_ω control the rate at which the closure coefficients approach their fully turbulent values. As in previous analyses based on the k-ω model,[7,8,9] we can determine their values by using perturbation methods to analyze the viscous sublayer. Using the well established procedure, we can solve for the constant in the law of the wall, B, by solving the sublayer equations and evaluating the following limit.

$$B = \lim_{y \to \infty} [u^+ - \frac{1}{\kappa} \ln y^+] \tag{43}$$

where $u^+ = u/u_\tau$ and $y^+ = u_\tau y/\nu$ are standard sublayer scaled coordinates. Also, $\kappa = 0.41$ is Kármán's constant. For a given value of R_β and R_k, there is a unique value of R_w that yields a constant in the law of the wall of 5.0. For small values of R_β the peak value of k near the surface is close to the value achieved without viscous corrections, viz, $u_\tau^2/(\beta^*)^{\nu}$. As R_β increases, the maximum value of k near the surface increases. Comparison of computed sublayer structure with Direct Numerical Simulation (DNS) results of Mansour, et al[10] indicates the optimum choice for these three coefficients is as indicated in Equation (14). Section IV presents a complete comparison of computed channel flow properties with the Mansour, et al DNS results.

The only flaw in the model's asymptotic consistency occurs in the Reynolds shear stress, τ_{xy}. While the exact asymptotic behavior is $\tau_{xy} \sim y^3$, the model as formulated predicts $\tau_{xy} \sim y^4$. This discrepancy could easily be removed with another viscous modification. However, results obtained to date indicate this is of no significant consequence. It has no obvious bearing on either the model's ability to predict transition or properties of interest in turbulent boundary layers. The additional complexity and uncertainty involved in achieving this subtle feature of the very-near-wall behavior of τ_{xy} does not appear to be justified.

III. Difficulties Attending Use of the k-ε Model

Given the information developed in Section II, it is a simple matter to explain why little progress has been made in predicting transition with the k-ε model.[11] The primary difficulties can be easily demonstrated by focusing upon incompressible boundary layers. If we use the standard form of the k-ε model, Equations (17-19) are replaced by

$$u\frac{\partial k}{\partial x} + v\frac{\partial k}{\partial y} = \nu_T \left(\frac{\partial u}{\partial y}\right)^2 - \epsilon + \frac{\partial}{\partial y}\left[(\nu+\nu_T/\sigma_k)\frac{\partial k}{\partial y}\right] \quad (44)$$

$$u\frac{\partial \epsilon}{\partial x} + v\frac{\partial \epsilon}{\partial y} = C_{\epsilon1}\frac{\epsilon}{k}\nu_T \left(\frac{\partial u}{\partial y}\right)^2 - C_{\epsilon2}\frac{\epsilon^2}{k} + \frac{\partial}{\partial y}\left[(\nu+\nu_T/\sigma_\epsilon)\frac{\partial \epsilon}{\partial y}\right] \quad (45)$$

$$\nu_T = C_\mu f_\mu k^2 / \epsilon \quad (46)$$

Values of the closure coefficients/functions $C_{\epsilon1}$, $C_{\epsilon2}$, C_μ, f_μ, σ_k and σ_ϵ differ amongst the various versions of this model. In the absence of viscous modifications, the standard values used are $C_{\epsilon1} = 1.44$, $C_{\epsilon2} = 1.92$, $C_\mu = .09$, $f_\mu = 1$, $\sigma_k = 1$ and $\sigma_\epsilon = .769$.

One critical difference from the k-ω model is obvious by inspection of Equations (44-46). Specifically, if the turbulence energy is zero, ϵ must also be zero. We cannot simply drop the eddy viscosity in the ϵ equation because of the presence of k in the denominator of the ϵ equation's dissipation term. The model does possess a laminar-flow solution for the ratio of ϵ to k. That is, if we make the formal change of variables

$$\epsilon = C_\mu k \omega \quad (47)$$

and assume $\nu_T << \nu$, the following laminar-flow equation for ω results.

$$u\frac{\partial \omega}{\partial x} + v\frac{\partial \omega}{\partial y} = (C_{\epsilon1} - 1)f_\mu \left(\frac{\partial u}{\partial y}\right)^2 - (C_{\epsilon2} - 1)C_\mu \omega^2 + \nu\frac{\partial^2 \omega}{\partial y^2}$$
$$+ \frac{2\nu}{k}\frac{\partial k}{\partial y}\frac{\partial \omega}{\partial y} \quad (48)$$

Equation (48) is nearly identical to the limiting form of Equation (18) for $\nu_T/\nu \to 0$. The only significant difference is the last term on the right-hand side of Equation (48). Except close to the surface where k must be exactly zero, this term is unlikely to have a significant effect on the solution for small nonzero values of k. However, in a numerical solution, products of dependent-variable gradients are generally destabilizing, and the problem can only be aggravated by having a coefficient inversely proportional to k. This is not an insurmountable problem. However, establishing starting conditions is clearly more difficult with the k-ε model than with the k-ω model.

Given the diverse nature of viscous modifications that have been proposed for the k-ε model,[12] it is impossible to make any universal statements about why a specific model fails to predict realistic transition Reynolds numbers. Perhaps the strongest statement that can be made is, *no one has approached the problem from the transition point of view*. Most researchers have sought only to achieve asymptotic consistency and attempted transition predictions only as an afterthought. We can gain some insight by examining the net production per unit dissipation terms for the k and ϵ equations that are analogous to Equations (29) and (30), viz,

$$P_k = \frac{f_\mu}{C_\mu}Re_x \left(\frac{\partial F/\partial \eta}{W}\right)^2 - 1 \quad (49)$$

$$P_\epsilon = \frac{C_{\epsilon1}f_\mu}{C_{\epsilon2}C_\mu}Re_x \left(\frac{\partial F/\partial \eta}{W}\right)^2 - 1 \quad (50)$$

On the one hand, without viscous damping, if we assume Equation (31) is valid, we find $(Re_x)_k = 8,100$ and $(Re_x)_\epsilon = 10,800$. Consequently, like the high-Reynolds-number version of the k-ω model, transition will occur at too low a Reynolds number.

On the other hand, because f_μ, $C_{\epsilon2}$ and sometimes $C_{\epsilon1}$ are often permitted to be functions of distance from the surface and/or functions of Re_T, we cannot simply use Equation (31). Furthermore, some modelers add terms to the k and ϵ equations in addition to damping the closure coefficients. Each set of values for the closure coefficients and additional terms must be used in solving Equation (48) to determine the laminar-flow solution for ϵ/k. While it is clearly impossible to make a quantitative evaluation of all variants of the k-ε model, we can nevertheless make some general observations.

From the analysis of the k-ω model, it is obvious that having $f_\mu < 1$ will tend to delay transition. Virtually all modelers implement an f_μ that will accomplish this end. However, the modifications of Jones and Launder,[11] Chien,[13] and Lam and Bremhorst,[14] for example, damp $C_{\epsilon2}$ to the extent that $(Re_x)_\epsilon$ is smaller than $(Re_x)_k$. This is the opposite of what is needed and will have an undesirable effect on both the onset of and the extent of the transition region.

This discussion is not intended as an exhaustive survey of the numerous low-Reynolds-number versions of the k-ε model. Rather, it is intended to illustrate how difficult it is to apply the model to the transition problem. Given enough additional closure coefficients and damping functions, the k-ε model can probably be modified to permit satisfactory transition predictions. However, even if this is done, establishing starting conditions will ultimately require a solution to Equation (48). That is, to initialize the computation, we must effectively transform to the k-ω model. Since this is the natural starting point, it seems illogical to perform subsequent computations in terms of k and ϵ.

IV. Turbulent Flow Applications

To achieve a complete description of the transition from laminar to turbulent flow, we must be able to accurately describe the flow in the turbulent regime. This is, after all, the primary advantage of using turbulence model equations to describe transition. In this section, we examine channel and pipe flow to demonstrate how well the low-Reynolds-number form of the k-ω model predicts properties of turbulent flows.

Figures 1 and 2 compare computed channel-flow skin friction, c_f with the Halleen and Johnston[15] correlation for Reynolds number based on channel height, H, and average velocity ranging from 10^3 to 10^5. The correlation is

$$c_f = 0.0706 \, Re_H^{-\frac{1}{4}} \tag{51}$$

As shown, computed c_f differs from the correlation by less than 3% except at the lowest Reynolds number shown where the correlation probably is inaccurate. Figure 3 compares computed pipe flow c_f with Prandtl's universal law of friction, viz,

$$c_f^{-\frac{1}{2}} = 4 \log_{10}(2 \, Re_D \, c_f^{\frac{1}{2}}) - 1.6 \tag{52}$$

Reynolds number based on pipe diameter, D, and average velocity varies from 10^3 to 10^6. As with channel flow, computed c_f falls within 5% of the correlation except at the lowest Reynolds number indicated where the correlation is likely to be in error.

For more detailed comparisons, we consider two low-Reynolds-number channel-flow cases corresponding to the DNS results of Mansour, et al[10] and one high-Reynolds-number pipe flow case corresponding to measurements of Laufer[16].

For purposes of identification, the three cases are referred to in terms of the parameter

$$Re_\tau = u_\tau R / \nu \tag{53}$$

where u_τ is friction velocity and R is either channel half height or pipe radius. Figures 1 and 2 compare various computed profiles with the Mansour, et al DNS results for Re_τ = 180 and 395, respectively.

Six different comparisons are shown in each figure, including mean velocity, skin friction, Reynolds shear stress, turbulence kinetic energy, turbulence energy production and dissipation rate. For both cases, velocity, Reynolds shear stress, and turbulence kinetic energy profiles differ by less than 7%. Most notably, for both Reynolds numbers, the model predicts the peak value of k near the channel wall to within 4% of the DNS value. Additionally, approaching the surface, the turbulence-energy production, $\tau_{xy} \partial U / \partial y$, and dissipation, ϵ, are within 10% of the DNS results except very close to the surface.

Figure 3 compares k-ω model pipe flow results with Laufer's[16] measurements at a Reynolds number based on pipe diameter and average velocity of 40,000. As shown, computed and measured velocity and Reynolds shear stress profiles differ by less than 8%. As with channel flow, computed and measured turbulence kinetic energy differ by about 5% including close to the surface where the sharp peak occurs. Note that, at this high a Reynolds number, the k profile has a sharp spike near y = 0 and this feature is captured in the computations. Except very close to the surface, computed turbulence energy production and dissipation differ from measured values by less than 10%. This may actually be a desirable result. That is, some controversy exists about the accuracy of Laufer's dissipation measurements close to the surface.
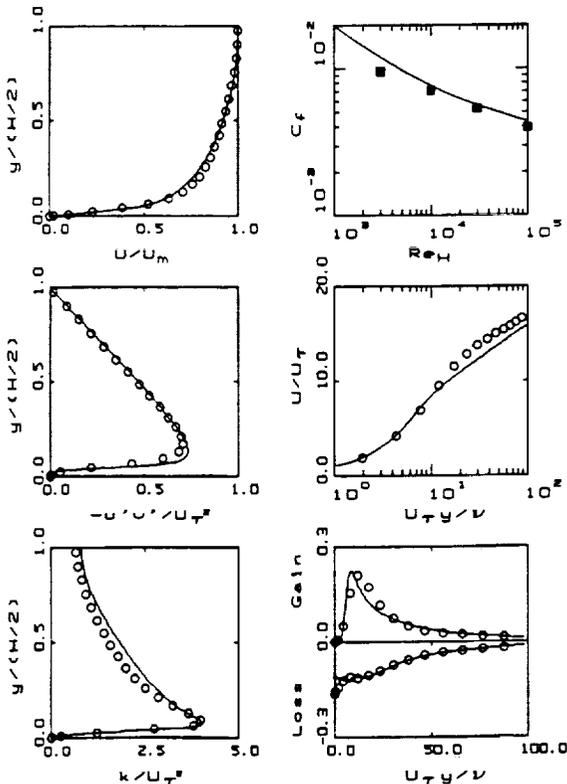
Figure 1. Incompressible channel flow with Re_τ = 180, Re_H = 5,590; o Mansour, et al; ▪ Johnston Formula.
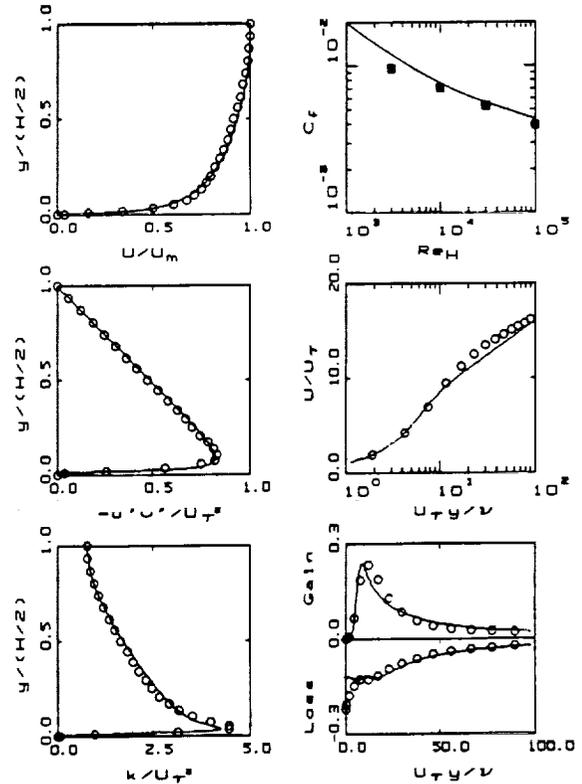
Figure 2. Incompressible channel flow with Re_τ = 395, Re_H = 13,750; o Mansour, et al; ▪ Johnston Formula.
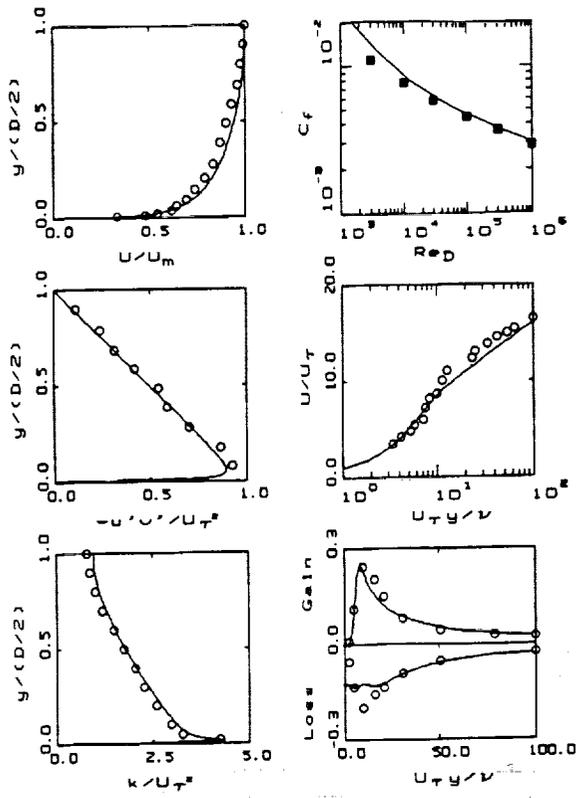
Figure 3. Incompressible pipe flow with $Re_\tau = 1058$, $Re_H = 40,000$; o Laufer; ■ Prandtl Formula.

Figure 4. Comparison of computed and measured variation of transition Reynolds number with freestream turbulence intensity; incompressible flat-plate boundary layer.

Figure 5. Comparison of computed and measured width of the transition region for an incompressible flat-plate boundary layer.

V. Transition Applications

Figure 4 compares computed and measured transition Reynolds number, Re_{θ_t}, for an incompressible flat-plate boundary layer. We define the transition Reynolds number as the point where the skin friction achieves its minimum value. Results are displayed as a function of freestream turbulence intensity, T', defined by

$$T' = 100 \left(\frac{2}{3} \frac{k_e}{U_e^2}\right)^{1/2} \qquad (54)$$

where subscript e denotes the value at the boundary-layer edge. As shown, consistent with the data compiled by Dryden,[17] Re_{θ_t} increases as the freestream intensity decreases. Because ω can be thought of as an averaged frequency of the freestream turbulence, it is reasonable to expect the predictions to be sensitive to the freestream value of ω. To assess the effect, the freestream value of the turbulence length scale defined by $\ell = k^{1/2}/\omega$ has been varied from $.001\delta$ to $.100\delta$ where δ is boundary layer thickness. As shown, computed Re_{θ_t} values bracket virtually all of the data. These predictions are markedly superior to the preliminary efforts of Wilcox[16] in developing low-Reynolds-number modifications for the k-ω model.

Figure 5 compares computed width of the transition region with measurements of Dhawan and Narasimha.[19] We define transition width, Δx_t, as the distance between minimum and maximum skin-friction points. The computed width falls within experimental data scatter for $Re_{x_t} < 10^6$, and lies a bit above the data for larger values. Δx_t is unaffected by the freestream value of ω.

VI. Summary and Conclusions

The primary objective of this paper has been to illustrate how two-equation turbulence models, most notably the k-ω model, predict transition. While the long-term goal of this research is to develop a transition model for all Mach numbers, this paper has focused on the case about which we know the most, viz, incompressible flow. The low-Reynolds-number modifications proposed not only facilitate accurate transition predictions, but also yield reasonably close agreement with DNS results for low-Reynolds-number channel flow.

The degeneracy of the ϵ equation in the k-ϵ model is a major stumbling block that impedes successful application

to the transition problem. By transforming the model to an equivalent k-ω model, it would be possible to remove some of the difficulties. After making such a transformation however, there is little reason to transform back.

The applications presented in Sections IV and V indicate we have formed a solid foundation for future low-Reynolds-number and transition research.

VII. Acknowledgements

References

[1]Wilcox, D. C., "Turbulence-Model Transition Predictions," AIAA Journal, Vol. 13, No. 2, pp. 241-243 (1975).

[2]Wilcox, D. C., "Turbulence Model Transition Predictions: Effects of Surface Roughness and Pressure Gradient," AIAA Paper 75-857, Hartford, CT (1975).

[3]Wilcox, D. C. and Chambers, T. L., "Application of the Turbulence-Model Transition-Prediction Method to Flight Test Vehicles," Turbulence in Internal Flows, S.N.B. Murthy, pp. 233-247 (1976).

[4]Wilcox, D. C., "A Model for Transitional Flows," AIAA Paper 77-126, Los Angeles, CA (1977).

[5]Wilcox, D. C., "Alternative to the e^9 Procedure for Predicting Boundary-Layer Transition," AIAA Journal, Vol. 19, No. 1, pp. 56-64 (1981).

[6]Wilcox, D. C. and Marvin, J. G., "Combined Effects of Freestream Turbulence and Mass Addition on Blunt-Body Heating and Transition," Proceedings of the 2nd ASME/JSME Joint Thermal Engineering Conference, Honolulu, HI (1987).

[7]Wilcox, D. C., "Reassessment of the Scale Determining Equation for Advanced Turbulence Models," AIAA Journal, Vol. 26, No. 11, pp. 1299-1310 (1988).

[8]Wilcox, D. C. and Traci, R. M., "A Complete Model of Turbulence," AIAA Paper 76-351, San Diego, CA (1976).

[9]Wilcox, D. C. and Rubesin, M. W., "Progress in Turbulence Modeling for Complex Flow Fields Including Effects of Compressibility," NASA TP 1517 (1980).

[10]Mansour, N. N., Kim, J. and Moin, P., "Reynolds Stress and Dissipation Rate Budgets in Turbulent Channel Flow," JFM, Vol. 194, pp. 15-44 (1988).

[11]Jones, W. P. and Launder, B. E., "The Prediction of Laminarization with a Two-Equation Model of Turbulence," International Journal of Heat and Mass Transfer, Vol. 15, pp. 301-314 (1972).

[12]Patel, V. C., Rodi, W. and Scheuerer, G., "Turbulence Models for Near-Wall and Low Reynolds Number Flows: A Review," AIAA Journal, Vol. 23, pp. 1308-1319 (1985).

[13]Chien, K-Y., "Predictions of Channel and Boundary-Layer Flows with a Low-Reynolds-Number Turbulence Model," AIAA Journal, Vol. 20, pp. 33-38 (1982).

[14]Lam, C. K. G. and Bremhorst, K. A., "Modified Form of the k-ε Model for Predicting Wall Turbulence," Journal of Fluids Engineering, Vol. 103, pp. 456-460 (1981).

[15]Halleen, R. M. and Johnston, J. P., "The Influence of Rotation on Flow in a Long Rectangular Channel - An Experimental Study," Report MD-18, Mechanical Engineering Dept., Stanford University (1967).

[16]Laufer, J., "The Structure of Turbulence in Fully Developed Pipe Flow," NACA 1174 (1952).

[17]Dryden, H. L., Aerodynamics and Jet Propulsion, Vol. V, University Press, Princeton, NJ (1959).

[18]Wilcox, D. C., "Progress in Hypersonic Turbulence Modeling," AIAA Paper 91-1785, Honolulu, HI (1991).

[19]Dhawan, S. and Narasimha, R., "Some Properties of Boundary Layer Flow During the Transition from Laminar to Turbulent Motion," JFM, Vol. 3, pp. 418-436 (1958).